ELSEVIER

Journal of Power Sources 113 (2003) 166–172

JOURNAL OF POWER SOURCES

www.elsevier.com/locate/jpowsour

Tris(2,2,2-trifluoroethyl) phosphite as a co-solvent for nonflammable electrolytes in Li-ion batteries

S.S. Zhang*, K. Xu, T.R. Jow

US Army Research Laboratory, Sensors and Electron Devices Directorate, Adelphi, MD 20783-1197, USA

Received 16 September 2002; accepted 24 September 2002

Abstract

In this work, we used tris(2,2,2-trifluoroethyl) phosphite (TTFP), in which the oxidization number of phosphorus was three (III), to formulate nonflammable electrolytes of the Li-ion batteries. Using 1 m (mole solute per kilogram solvent) $LiPF_6$ 3:3:4 (w) propylene carbonate (PC)/ethylene carbonate (EC)/ethyl methyl carbonate (EMC) electrolyte as a baseline, the effect of TTFP on the flammability and conductivity of the electrolytes, as well as the cell performance was evaluated. It is observed that the addition of TTFP can substantially reduce flammability of the electrolytes at a small expense in the ionic conductivity. When the TTFP content reaches 15 wt.% versus the solvent, the electrolyte becomes nonflammable. In Li/graphite half-cell, TTFP not only suppresses PC decomposition and graphite exfoliation but also increases Coulombic efficiency (CE) of the lithiation and delithiation cycle. In Li/cathode (a lithium nickel-based mixed oxide cathode) half-cell, TTFP has negligible adverse impact on the cycling performance when the cells are cycled between 2.7 and 4.2 V. In graphite/cathode Li-ion cell using PC-based electrolytes, TTFP can improve cycling performance, especially at high temperature (60 °C), since its presence favors the formation of solid electrolyte interface (SEI) film on the graphite electrode and increases thermal stability of $LiPF_6$-based electrolytes.

Keywords: Li-ion battery; Nonflammable electrolyte; Phosphite; Phosphate; Fire retardant

1. Introduction

Safety concerns have been an obstacle for the development of large-size Li-ion batteries and high power battery modules, which are needed in the application of electric vehicle (EV) and hybrid electric vehicle (HEV). Major sources for the safety hazards were reported to arise from the chemical reactions between electrode materials and electrolyte constitutes at high temperatures [1–8]. These reactions are known to be very exothermic and are often induced under abuse conditions, such as overcharge/discharge, short circuit, and operation at high temperatures. The generated heat in turn can exponentially accelerate the reactions and cause catastrophic thermal runway, i.e. a self-sustaining increase in cell heating. As a result, the cell can be violently vented and the flammable electrolyte solvents can be ignited to combust, which results in safety hazards.

To improve the safety of Li-ion batteries, much effort has been focused on the development of nonflammable electrolytes [9–21]. The most acceptable approach is to add directly fire-retardants as a co-solvent (or called additive) into the normal liquid electrolytes [9–16]. Most of the reported fire-retardants are organophosphous compounds, such as phosphates [9–15,17,18] and phosphazenes [10,14,16]. With very limited information available, few are based on the idea that the fire-retardant solvents generate fire-retarding gases, such as CO_2, SO_3, N_2, upon thermal decomposition [10,14]. It has been found that most of the above fire-retardants affect battery performance due to their reactivity with the electrode active materials with few exceptions [13,15]. An alternative approach is to develop nonflammable solid or gel polymer electrolytes [17–21], in which either fire-retarding additives [17,18] or less flammable polymers [19,21] are used. However, polymer electrolyte technology is restricted in the fabrication of the large-size Li-ion batteries since fabrication needs a moisture-free environment and the batteries are in an electrolyte-activated state as assembled.

In our recent work [22], we have found that tris(2,2,2-trifluoroethyl) phosphite (TTFP), in which the oxidization number of phosphorus is three (III) instead of five (V), is very effective in improving the thermal stability of $LiPF_6$-based electrolytes. That is, 0.2–1.0 wt.% of TTFP is enough

* Corresponding author. Tel.: +1-301-394-0981; fax: +1-301-394-0273.
E-mail address: szhang@arl.army.mil (S.S. Zhang).

0378-7753/02/$ – see front matter
PII: S0378-7753(02)00537-2

to suppress thermal decomposition of $LiPF_6$ in a non-aqueous electrolyte. Furthermore, TTFP is electrochemically stable against the oxidation on the cathode surface and it also can inhibit PC decomposition in Li/graphite half-cell. In this paper, we will report the property of TTFP in reducing flammability of the liquid electrolytes of Li-ion batteries and discuss its impact on the battery performance.

2. Experimental

$LiPF_6$ (>99.9%, Stella Chemifa Corp.), ethylene carbonate (EC) and propylene carbonate (PC, both are battery grade and from Grant Chemical) were used as received. Ethylmethyl carbonate (EMC, water content <30 ppm, Mitsubishi Chemical Co.) and tris(2,2,2-trifluoroethyl) phosphite (TTFP, Aldrich, 99%) were dried using activated aluminum oxide before use. Electrolytes with various compositions were prepared in an argon-filled glove box. A weight ratio was used to describe the composition of all solvent mixtures, and the content of TTFP in the electrolytes was expressed as a weight percentage versus the solvent mixture instead of the electrolyte. Self-extinguishing time (SET) normalized against the liquid electrolyte mass was used to evaluate the flammability of the electrolytes. It was obtained by igniting a pre-weighed electrolyte solution soaked in a porous wick, followed by recording the time it took for the flame to extinguish. The details about the testing procedure and result reliability have been described elsewhere [13]. Solartron SI 1287 Electrochemical Interface and SI 1260 Impedance/Gain-Phase Analyzer, controlled by Zplot software, were used to determine ionic conductivity of the electrolytes by measuring impedance of the electrolytes in a two-platinum-electrode cell having a cell constant of 1.586 cm^{-1}.

Graphite and cathode (a lithium nickel-based mixed oxide cathode, and hereinafter called as "cathode") films were supplied by SAFT America Inc., and dried at 110 °C for 16 h under vacuum before use. For cell assembly, graphite and cathode films were cut into disc of 1.27 and 0.97 cm^2, respectively. In a dry room with a dew point of about −70 °C, Li/graphite, Li/cathode, and graphite/cathode 2335-type button cells were assembled and filled with 150 μl of electrolyte. Cycling tests of the cells were performed on a Maccor Series 4000 tester and the cycling conditions will be described in the discussion or figure captions. High temperature storage performance of the cells was evaluated in a Tenney Environmental Oven Series 942 by recording open-circuit voltage (OCV) change of the cells versus the storage time.

3. Results and discussion

3.1. Effect of TTFP on flammability and conductivity

In order to distinguish tris(2,2,2-trifluoroethyl) phosphite (TTFP) from other organophosphous(V) compounds, especially tris(2,2,2-trifluoethyl) phosphate (TFP) that we have reported as a fire-retardant [15], we first show the chemical structure of TTFP below:

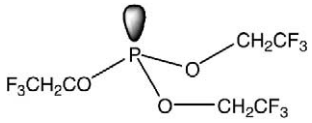

where the oxidization number of phosphorus is three (III) and the phosphorus center atom bears a pair of lone-pair electrons. TTFP by itself is nonflammable and is miscible with PC in any ratio. However, it is rather immiscible with EC due probably to its relatively low polarity.

To examine the fire-retardant ability of TTFP in the liquid electrolytes of Li-ion batteries, we selected 1 m $LiPF_6$ 3:3:4 PC/EC/EMC electrolyte as a baseline. This selection was based on the following reasons: (i) from the standpoint view of thermodynamics, ternary mixed solvent can achieve much lower liquidus temperature than the binary one does; (ii) the presence of PC favors super-cooling, which is helpful for low temperature operation of the Li-ion cells; and (iii) partial replacement of either volatile EMC or readily crystallized EC (m.p. = 36 °C) with PC, which has low m.p. (−49 °C) and high b.p. (242 °C), is desirable for the safety and low temperature operation of the Li-ion batteries. Fig. 1 shows an effect of TTFP on the SET and ionic conductivity (at 24 °C) of the electrolyte, in which the SET is an averaged value obtained from at least five individual tests. We see that the control electrolyte is very flammable, as indicated by an infinite SET of more than 50 s/g. However, with addition of TTFP into the electrolyte, SET of the electrolyte is substantially reduced. As suggested by an SET of near zero, the electrolyte becomes nonflammable when the TTFP content reaches 15% or higher. As an adverse effect, we notice that the ionic conductivity of the electrolyte is monotonically decreased with an increase in the TTFP content. This

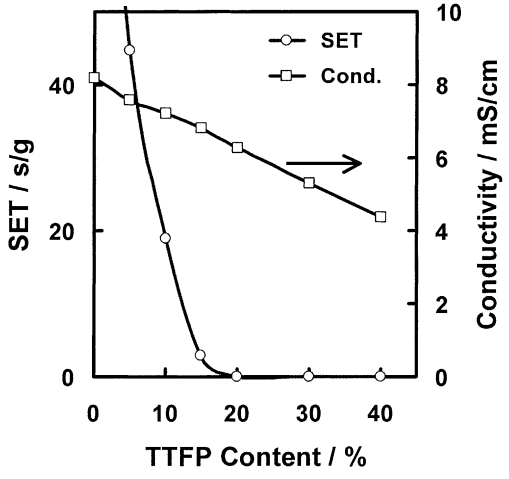

Fig. 1. Effect of TTFP on the flammability and ionic conductivity (24 °C) of 1 m $LiPF_6$ 3:3:4 PC/EC/EMC electrolyte.

phenomenon can be ascribed to the low dielectric constant (i.e. polarity) of TTFP, which suppresses dissociation of the salt. As an evidence of the low dielectric constant, we have observed that $LiPF_6$ is insoluble in TTFP sole solvent. From above results, we conclude that 15–20% of TTFP would be enough to form a nonflammable electrolyte of the Li-ion batteries with the ionic conductivity retaining over 80% of the control value.

3.2. Li/graphite half-cell

Our previous work [24] showed that the graphite electrode used in this study performs well in a 1 m $LiPF_6$ 1:1:3 PC/EC/EMC electrolyte, however, it fails to perform in the present one (1 m $LiPF_6$ 3:3:4 PC/EC/EMC) without use of electrolyte additive or modification of graphite surface. As a result of PC decomposition and graphite exfoliation, the Li/graphite half-cell using the control electrolyte could not be discharged down to 0.5 V in the first lithiation process. We recently found [19] that TTFP is capable of suppressing PC decomposition since TTFP can be electrochemically reduced at higher potentials (∼1.8 V versus Li^+/Li), which helps to form a protective solid electrolyte interface (SEI) film on the surface of graphite electrode. Therefore, we used 1 m $LiPF_6$ 3:3:4 PC/EC/EMC electrolyte to examine the electrochemical stability of TTFP against the lithiated graphite.

Fig. 2 shows cycling performance of the first cycle for a series of Li/graphite half-cells. Due to PC decomposition and graphite exfoliation, the control cell failed to perform (not shown in Fig. 2). It is shown in Fig. 2a that, with addition of TTFP (even only 5%) into the electrolyte, all the Li/graphite half-cells can pass the voltage regions of 0.6–0.8 V, in which PC is generally decomposed in the absence of TTFP, and continuously fall until the pre-set limiting voltage (0.002 V) is reached. We see that the lithiated graphite can be reversibly delithiated when the cells are subsequently charged. The above observations reveal that TTFP is able to facilitate the lithiation and delithiation cycle of graphite with 3:3:4 PC/EC/EMC mixed solvents, which otherwise fails to perform.

To better observe the effect of TTFP on the lithiation and delithiation cycle of graphite, we plot differential capacities of the Li/graphite half-cells versus the voltage in Fig. 2b, in which the numbers present Coulombic efficiency (CE) of the first cycle of each cell. We see that all these cells display three pairs of reversible differential capacity peaks between 0.30 and 0.002 V. This reflects a typically electrochemical characteristic of the intercalation and deintercalation of Li^+ ion with graphite, which is known to correspond to three major phase–phase transitions of the lithium graphite insertion compounds [23,24]. More interestingly, the CE of the lithiation and delithiation cycle is found to increase with the TTFP content (see the numbers in Fig. 2b). As mentioned above, graphite fails to cycle in the control electrolyte due to PC decomposition. However, with adding of 5% TTFP into the electrolyte, not only graphite withstands the cycling, but

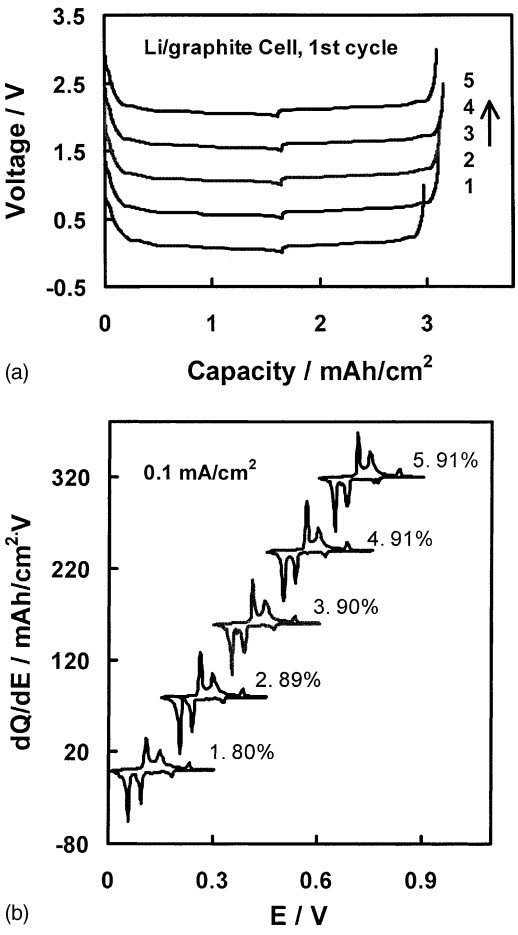

Fig. 2. Cycling performance of the Li/graphite half-cells with 1 m $LiPF_6$ 3:3:4 PC/EC/EMC electrolyte containing TTFP content of (1) 5%, (2) 10%, (3) 15%, (4) 20%, (5) 30%, respectively, which was obtained from the first cycle at 0.1 mA/cm^2 between 0.002 and 1.0 V. (a) Voltage–capacity curves, in which each plot was shifted (0 mAh/cm^2, +0.5 V) from the last one for the purpose of graph clarity, (b) Differential capacities vs. the voltage, in which each plot was shifted (+0.15 V, +80 mAh/cm^2 V) from the last one and the numbers show Coulombic efficiency of each cell.

also the CE reaches as high as 80% (plot 1). Furthermore, the CE increases to 89% when the TTFP content is 10%. After this, the CE no longer increases with the TTFP content, which means that ∼10% of the irreversible capacities would be the necessary value for the formation of SEI film on the graphite surface. For example, even using 1 m $LiPF_6$ 3:7 EC/EMC electrolyte, in which PC is not present, the counterpart Li/graphite half-cell still shows a 13% of irreversible capacities in the first cycle [24].

Chemical stability of TTFP against the lithiated graphite can be determined by simply observing the open-circuit voltage (OCV) change of a fully discharged (lithiated) Li/graphite half-cell. Fig. 3 shows the OCV of a fully discharged Li/graphite half-cell, with the electrolyte containing 20% of TTFP, as a function of the storage time at 60 °C. It is seen that the OCV is slowly increased with the storage time through three voltage plateaus, in which the third plateau stage is still not completed by the end of the experiment.

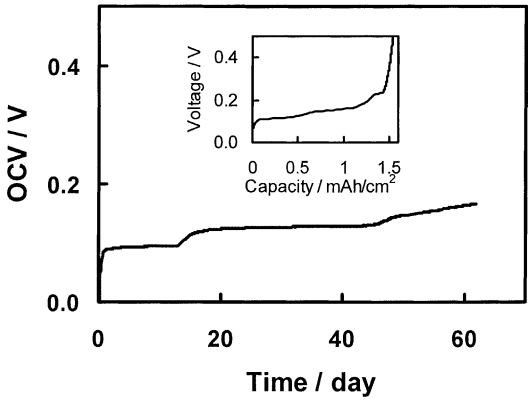

Fig. 3. Open-circuit voltage increase of a fully discharged Li/graphite half-cell with 1 m $LiPF_6$ 3:3:4 PC/EC/EMC electrolyte containing 20% of TTFP at 60 °C. Inset shows a regular voltage–capacity curve of the charge (delithiation) process of the same cell.

This behavior is very similar to the voltage–capacity curve of a normal charge (delithiation) process of the Li/graphite half-cell, as shown in the inset. Considering the IR drop caused during a practical charge process of the Li/graphite half-cell, one may notice that the voltage regions of each plateau in Fig. 3 and in the inset, respectively, are very consistent with each other. Furthermore, we found that the capacity loss during the storage can be recovered in the following lithiation. Therefore, we consider that the observed OCV increase in Fig. 3 is a simple self-delithiation process, which corresponds to a self-discharge process in the practical Li-ion battery and can be described by this equation:

$$Li_xC_6 \rightarrow Li_{x-\delta}C_6 + \delta Li^+ + \delta e \quad (1)$$

There are two possible mechanisms, which are related to the self-delithiation of the Li/graphite half-cell. One is a local redox process due to the reactions between the electrode and electrolyte components, which have been observed not only from the Li/graphite cell [25] but also from the $Li/LiMn_2O_4$ cell [26,27]. That is, graphite delithiation and electrolyte reduction simultaneously take place in the vicinity of the graphite electrode. The other one is an internal "shuttle" redox process [28], which is usually caused by the reduction and oxidization of electroactive impurities in the anode and cathode, respectively. From the point view of electrochemistry, the self-delithiation caused by the above two processes is reversible and its related capacity loss is recoverable in the subsequent lithiation. In the present case, we consider that the observed self-delithiation in Fig. 3 more likely arises from the local redox processes.

3.3. Li/cathode half-cell

Effect of TTFP on the cathode performance is evaluated by cycling galvanostatically a series of Li/cathode half-cells with different TTFP contents. We observe that all the Li/cathode half-cells, containing TTFP from 0 to 30%, have an invariant CE of 83–86% in the first charge and discharge cycle. This implies that TTFP has negligible impact on the first cycle of the Li/cathode half-cell. Our recent study [29] showed that the irreversible capacities observed from the first cycle of the cathode (lithium nickel-based mixed oxide) mainly originate from these two irreversible processes of (i) structural change of the cathode material and (ii) reactions of the cathode active material and electrolyte solvents, in which only the latter is affected by the electrolyte components. Therefore, we conclude from the nearly constant CE of the first cycle that TTFP would be suitable as an electrolyte co-solvent for the Li/cathode half-cell.

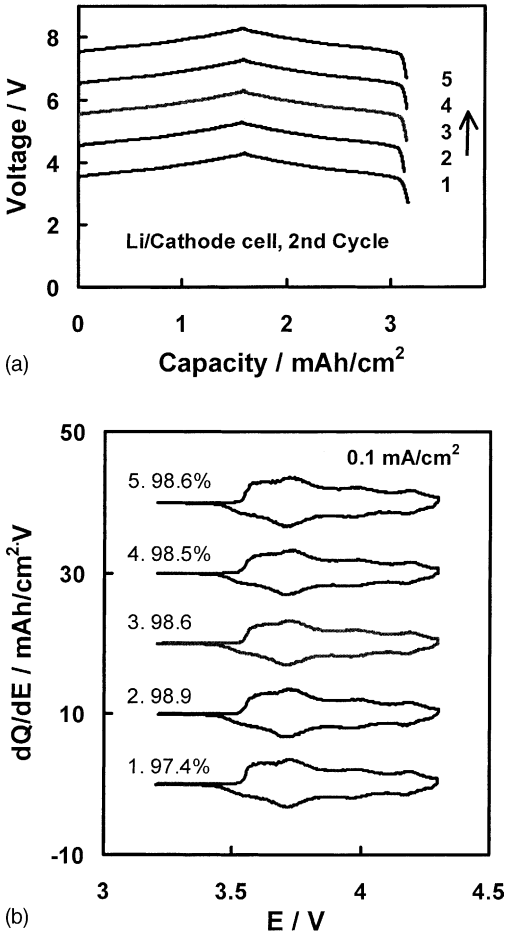

Fig. 4. Cycling performance of the Li/cathode half-cells with 1 m $LiPF_6$ 3:3:4 PC/EC/EMC electrolyte containing TTFP content of (1) 0%, (2) 10%, (3) 15%, (4) 20%, (5) 30%, respectively, which was obtained from the second cycle at 0.1 mA/cm^2 between 2.7 and 4.3 V. (a) Voltage–capacity curves, in which each plot was shifted (0 mAh/cm^2, +1.0 V) from the last one. (b) Differential capacities versus the voltage, in which each plot was shifted (0 V, +10 mAh/cm^2 V) from the last one and the numbers show Coulombic efficiency of each cell.

Voltage–capacity curves and differential capacities versus the voltage for the second cycle of the Li/cathode half-cells containing different TTFP contents are plotted in Fig. 4. We see that all five cells show nearly identical voltage–capacity profile (Fig. 4a) and that their differential capacities present

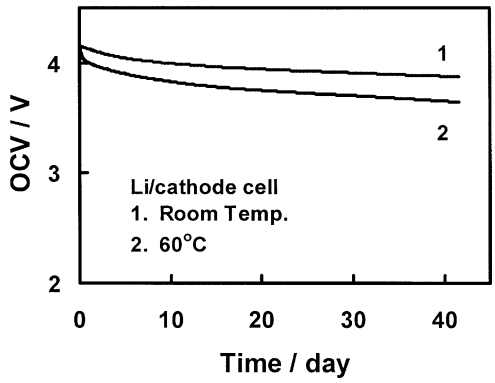

Fig. 5. Open-circuit voltage decline of the fully charged Li/cathode half-cells with 1 m $LiPF_6$ 3:3:4 PC/EC/EMC electrolyte containing 20% of TTFP (1) at room temperature and (2) at 60 °C.

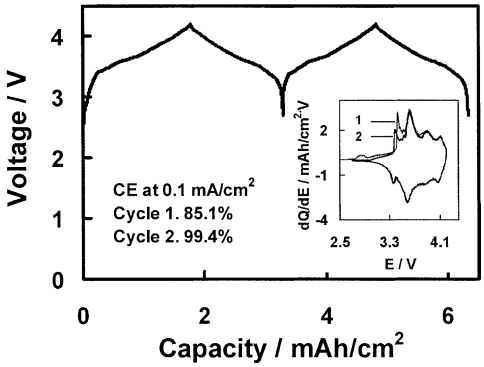

Fig. 6. Voltage–capacity curve of a graphite/cathode Li-ion cell with 1 m $LiPF_6$ 3:3:4 PC/EC/EMC electrolyte containing 20% of TTFP, which was recorded from the first two cycles at 0.1 mA/cm^2 between 2.7 and 4.1 V. Inset shows differential capacities versus the voltage of these two cycles.

three pairs of wide and overlapped peaks with the voltage change (Fig. 4b), which reflects an universally electrochemical feature of the lithium nickel-based mixed oxides, as reported elsewhere [30,31]. It is determined from Fig. 4a and shown in Fig. 4b that all these five cells have nearly invariant CEs of 97–99% in the second cycle.

Fig. 5 compares the OCV decline of two fully charged Li/cathode half-cells with the storage time at room temperature and 60 °C, respectively. Both cells were first charged to 4.2 V and then left standing at open-circuit for an hour to reach a stable OCV (4.12 V), followed by recording their OCV with the storage time on a Maccor tester. As Fig. 5 shows, OCVs of both cells is slowly decreased with the storage time. After 42 days, the OCV of the cell stored at room temperature dropped to 3.87 V, while the one at 60 °C to 3.64 V. In response to the observed OCV decline, we first concerned that the chemical stability of TTFP against the oxidation of the cathode might be a challenge. However, similar results also were obtained from many control cells. Therefore, we ascribe the OCV decline shown in Fig. 5 to a normal self-discharge process of the Li/cathode cells, which may be related to many factors, such as the local redox process as described above and the irreversible reactions between cathode active material and electrolyte solvents.

3.4. Graphite/cathode Li-ion cell

Using 1 m $LiPF_6$ 3:3:4 PC/EC/EMC electrolyte containing 20% of TTFP, a graphite/cathode Li-ion cell was assembled and cycled galvanostatically. Shown in Fig. 6 is a voltage–capacity curve of the first two cycles of the cell. It is calculated from Fig. 6 that the CE of the first two cycles is 85.1 and 99.4%, respectively. In order to find the voltage regions in which the irreversible capacities are really formed, we plot the differential capacities of these two cycles versus the voltage as an inset in Fig. 6. It can be observed from the inset that all the irreversible capacities are developed below 3.6 V during the first charging process, as suggested by the completely overlapped plots of the differential capacities versus the voltage in the rest voltage regions.

It is interesting to compare the CEs of the first cycle for the Li/graphite (91%), Li/cathode (84%), and graphite/cathode (85.1%) cells. We find that the CE of the graphite/cathode Li-ion cell is very close to the lower one of the Li/graphite and Li/cathode half-cells, which means that the irreversible capacities produced simultaneously on the graphite and cathode, respectively, during the first cycle must be complementary to each other. In other words, the formation of the irreversible capacities in the initial forming cycles of the Li-ion cell mainly involves an electrochemical decomposition of the electrolyte components (salt and solvents), which generally yields solid or gaseous products. It is known that the insoluble solid products lead to the formation of SEI film on graphite [24] and cathode [29] surface, respectively, while the gaseous products are present within the cells. To release these gaseous products, it is recommended that the Li-ion battery, especially the large-size ones, should be sealed after the initial forming cycles were completed.

The influence of TTFP on the cycling performances of graphite/cathode Li-ion cells is shown in Fig. 7. It appears that the discharge capacities of these cells are increased with the TTFP content in the electrolytes (Fig. 7a). Furthermore, capacity retention of the cells against the cycle number is improved by the addition of TTFP. These improvements might be due to that the presence of TTFP favors to form a batter SEI film. When the temperature is increased to 60 °C, the capacities of all these cells are accordingly increased as a result of an increase in the ionic conductivity of the electrolyte and SEI film. At 60 °C, the improved capacity retention of the cells by TTFP is still obvious (Fig. 7b).

Fig. 8 compares OCV change of the fully charged graphite/cathode Li-ion cells with the storage time at different storage temperatures. We see that at higher temperature, the OCV declines faster. This result is very similar as that observed in the Li/cathode half-cell (Fig. 5) and can be ascribed to self-discharge of the cell. For the purpose of

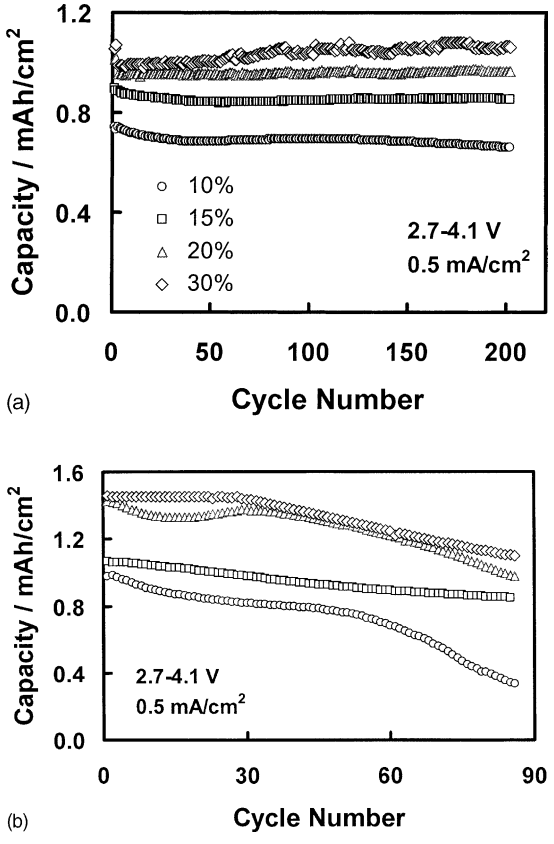

Fig. 7. Cycling performance of the graphite/cathode Li-ion cells with 1 m $LiPF_6$ 3:3:4 PC/EC/EMC electrolytes containing different TTFP content (a) at room temperature and (b) at 60 °C. Note that the data in (b) were continued from those of (a), and that the cell was cycled at 0.5 mA/cm^2 between 2.7 and 4.1 V.

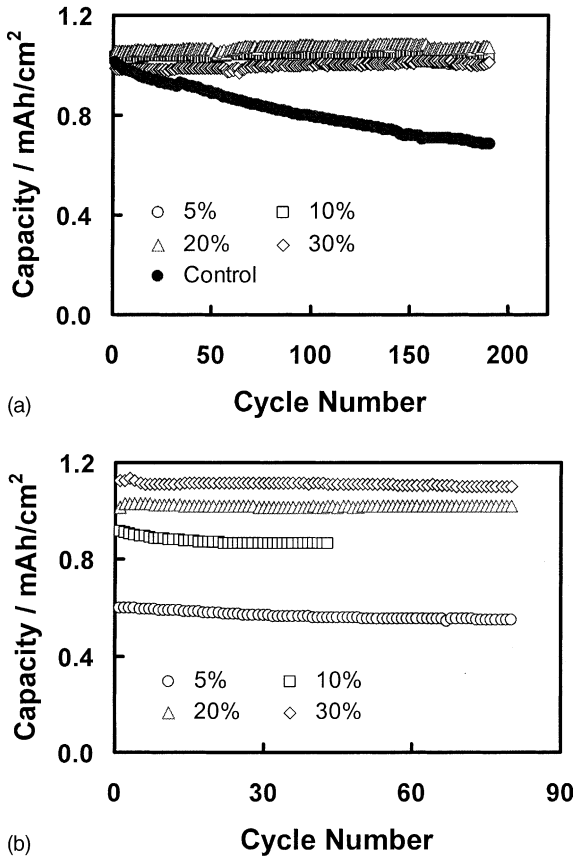

Fig. 9. Cycling performance of the graphite/cathode Li-ion cells with 1 m $LiPF_6$ 1:1:3 PC/EC/EMC electrolytes containing different TTFP contents (a) at room temperature and (b) at 60 °C. Note that the data in (b) were continued from those of (a), and that the cell was cycled at 0.5 mA/cm^2 between 2.5 and 3.9 V with a charge limiting time of 3 h.

comparison, OCV of the Li/cathode half-cell is also plotted in Fig. 8. It can be seen that, during 60 °C-storage, Li-ion cell (line 2) retains a more stable OCV than Li/cathode half-cell (line 3). Considering the fact that these two cells are made with the same electrolyte and cathode, one may attribute the stabilized OCV of Li-ion cell to the more stable graphite anode, in contrast to the rather reactive metal lithium anode in the Li/cathode half-cell. This benefit of the graphite anode can be further ascribed to the stable SEI film, which was formed in the presence of TTFP.

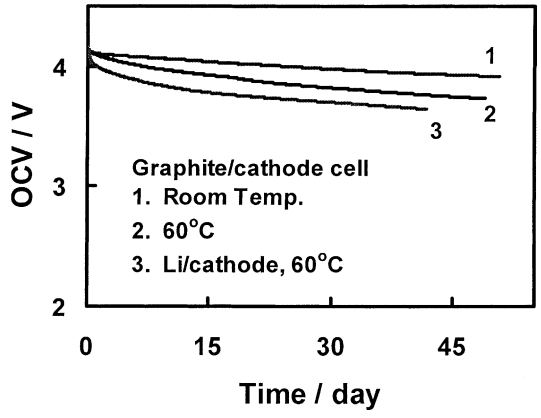

Fig. 8. Open-circuit voltage decline of the fully charged graphite/cathode Li-ion cells with 1 m $LiPF_6$ 3:3:4 PC/EC/EMC electrolyte containing 20% of TTFP (1) at room temperature and (2) at 60 °C. Line 3 is the data of Li/cathode half-cell at 60 °C, i.e. line 2 in Fig. 5, which is plotted for the purpose of comparison.

Cycling performances of the Li-ion cells with 1 m $LiPF_6$ 1:1:3 PC/EC/EMC based electrolytes are shown in Fig. 9, in which the cells were cycled between 2.5 and 3.9 V instead of between 2.7 and 4.1 V as used in Fig. 7. Due to a decrease in the PC content, the control cell is able to perform, however, its capacity decreases much faster (see control in Fig. 9a). Comparing Figs. 7a and 9a, one finds that, in 1:1:3 PC/EC/EMC mixed solvent, the capacity difference caused by the content of TTFP almost vanishes and the capacity against the cycle number becomes much more stable. Fig. 9a indicates that the cycling performance of the graphite/cathode Li-ion cell can be significantly improved by adding of 5% TTFP to the electrolyte. At 60 °C, these cells show more stable capacity retention (Fig. 9b), as compared to using a 3:3:4 PC/EC/EMC mixed solvent (Fig. 7b). However, the cells containing <20% of TTFP show rather low capacities. Therefore, we consider that 20% of TTFP might be necessary

for the improvement of cell performance and for the achievement of a nonflammable electrolyte.

4. Conclusions

In conclusion, tris(2,2,2-trifluoroethyl) phosphite (TTFP) is effective in reducing the flammability of the liquid electrolytes of Li-ion batteries. Addition of about 15% TTFP can make a 1 m $LiPF_6$ 3:3:4 PC/EC/EMC electrolyte nonflammable with the ionic conductivity retaining over 80% of the control value. An additional benefit is that TTFP can increase cycling efficiency of the graphite electrode in PC-based electrolytes by suppressing PC decomposition and graphite exfoliation. Furthermore, TTFP can improve the high temperature (60 °C) performance of the graphite/cathode Li-ion cells. Considering the effect of TTFP on the electrolyte flammability and cell performance, we consider that 15–20% is a reasonable range for the TTFP content. From Li/cathode and graphite/cathode 2335-type button cells, we have not observed any adverse impact of TTFP.

Acknowledgements

Receipt of the electrode films from SAFT America Inc. is gratefully acknowledged.

References

[1] Y. Chen, J.W. Evans, J. Electrochem. Soc. 143 (1996) 2708.
[2] A.D. Pasquier, F. Disma, T. Bowmer, A.S. Gozdz, G. Amatucci, J.M. Tarascon, J. Electrochem. Soc. 145 (1999) 472.
[3] J.S. Hong, H. Maleki, S.A. Hallaj, L. Redey, J.R. Selman, J. Electrochem. Soc. 145 (1998) 1489.
[4] H. Maleki, S.A. Hallaj, J.R. Selman, R.B. Dinwiddie, H. Wang, J. Electrochem. Soc. 146 (1999) 947.
[5] H. Maleki, G. Deng, A. Anaba, J. Howard, J. Electrochem. Soc. 146 (1999) 3224.
[6] M.N. Richard, J.R. Dahn, J. Electrochem. Soc. 146 (1999) 2068.
[7] M.N. Richard, J.R. Dahn, J. Electrochem. Soc. 146 (1999) 2078.
[8] S.C. Levy, P. Bro, Battery Hazards and Accident Prevention, Plenum Press, New York, 1994.
[9] K. Yokoyama, S. Fujita, A. Hiwara, Y. Naruse, M. Toriida, A. Omaru, US Patent 5,580,684 (1996).
[10] S.C. Narang, S.C. Ventura, B.J. Dougherty, M. Zhao, S. Smedley, G. Koolpe, US Patent 5,830,600 (1998).
[11] X.M. Wang, E. Yasukawa, S. Kasuya, J. Electrochem. Soc. 148 (2001) A1058.
[12] X.M. Wang, E. Yasukawa, S. Kasuya, J. Electrochem. Soc. 148 (2001) A1066.
[13] K. Xu, M.S. Ding, S.S. Zhang, J.L. Allen, T.R. Jow, J. Electrochem. Soc. 149 (2002) A622.
[14] S.C. Narang, S.C. Ventura, P. Cox, US Patent 6,168,885 B1 (2001).
[15] K. Xu, S.S. Zhang, J.L. Allen, T.R. Jow, J. Electrochem. Soc. 149 (2002) A1079.
[16] C.W. Lee, R. Venkatachalapathy, J. Prakash, Electrochem. Solid State Lett. 3 (2000) 63.
[17] I. Olsen, D.R. Shackle, US Patent 5,455,127 (1995).
[18] R.V. Morford, E.C. Kellam, M.A. Hofmann, R. Baldwin, H.R. Allcock, Solid State Ionics 133 (2000) 171.
[19] H. Akashi, US Patent 5,658,686 (1997).
[20] H. Akashi, K. Sekai, K.I. Tanaka, J. Electrochem. Soc. 145 (1988) 881.
[21] H. Akashi, K. Sekai, K.I. Tanaka, Electrochim. Acta 43 (1998) 1193.
[22] S.S. Zhang, K. Xu, T.R. Jow, Electrochem. Solid-State Lett. 5 (2002) A206.
[23] T. Ohzuku, Y. Iwakoshi, K. Sawai, J. Electrochem. Soc. 140 (1993) 2490.
[24] S.S. Zhang, M.S. Ding, K. Xu, J.L. Allen, T.R. Jow, Electrochem. Solid State Lett. 4 (2001) A206.
[25] A.M. Andersson, K. Edstrom, J. Electrochem. Soc. 148 (2001) A1100.
[26] D. Guyomard, J.M. Tarascon, J. Electrochem. Soc. 140 (1993) 3071.
[27] H. Huang, C.A. Vincent, P.G. Bruce, J. Electrochem. Soc. 146 (1999) 481.
[28] P. Arora, R.E. White, M. Doyle, J. Electrochem. Soc. 145 (1998) 3647.
[29] S.S. Zhang, K. Xu, T.R. Jow, Electrochem. Solid State Lett. 5 (2002) A92.
[30] A. Rougier, P. Gravereau, C. Delmas, J. Electrochem. Soc. 143 (1996) 1168.
[31] K.K. Lee, K.B. Kim, J. Electrochem. Soc. 147 (2000) 1709.